Propagation Model for Building Blockage in Satellite Mobile Communication Systems

Panayiotis A. Tirkas, *Member, IEEE*, Chad M. Wangsvick, *Student Member, IEEE*, and Constantine A. Balanis, *Fellow, IEEE*

***Abstract*—A propagation model for building blockage in satellite mobile communication systems is developed. This model characterizes the signal transmitted from a low-earth orbiting (LEO) satellite when there is an obstruction in the path of the signal. The obstruction is assumed to be a man-made structure. The analysis is performed using the uniform theory of diffraction (UTD). Using this method, both single and double diffractions from the structure edges were included. Direct and reflected rays from the ground and building were also included, whenever the satellite signal was not completely obstructed. The satellite is assumed to be moving along a circular orbit while the receiver is stationary. The normalized signal level (in decibels) and the signal attenuation rate (in decibels per second) are computed. Such information is considered very useful in developing the mobile system's hand-off algorithm.**

***Index Terms*—Geometrical theory of diffraction, satellite mobile communication.**

I. Introduction

RECENTLY introduced satellite mobile communication systems make use of low-earth orbiting (LEO) satellites [1]. There are considerable differences between land mobile and satellite mobile systems. One of these differences lies in the approach used to characterize the propagation environment. For land-based systems, the base station is fixed and has comparable height to the surrounding buildings. For LEO satellite systems, the satellites are moving at low altitude around the surface of the earth providing continuous coverage.

There are many propagation models published and verified by experiments for land-based systems. A review paper on this topic has recently been published by Bertoni *et al*. [2]. Similar propagation models for LEO satellite systems are limited to simple models and measurements [3], [4] and a combination of statistical and experimental models [5].

In this paper, the effect of blockage by buildings on the signal level from LEO satellite systems is examined using high-frequency ray-tracing methods. The analysis is performed using the uniform theory of diffraction (UTD) with single and double diffractions included. Also included in the propagation model are direct rays, reflected rays from the ground and building, and higher order reflected–diffracted rays. The normalized signal level (in decibels) versus satellite elevation angle and versus time is calculated. Also, the attenuation rate (in decibels per second) when the satellite descends behind a building is estimated and statistics of the attenuation rate for different building heights and mobile distances from the building are provided. The statistics obtained by this analysis are useful in the development of hand-off algorithms for satellite mobile communication systems. Hand-off to another satellite takes place whenever the signal level falls below an established threshold value. This ensures continuous coverage in cases where the signal transmitted from the satellite is blocked by a man-made structure such as a building.

Manuscript received July 9, 1996; revised March 10, 1997. This work was supported by Motorola, Inc., Satellite Communications Division, Chandler, AZ.

The authors are with the Department of Electrical Engineering, Telecommunications Research Center, Arizona State University, Tempe, AZ 85287 USA.

Publisher Item Identifier S 0018-926X(98)05775-5.

II. Propagation Model

The geometry of the propagation model is illustrated in Fig. 1. A LEO satellite moving in a circular orbit above the surface of the earth descends behind a row of buildings of height h_b and width w_b. A mobile antenna located at a height h_m above the ground is at a distance x_m away from the building. The received signal at the mobile antenna is estimated for satellite elevation angles of $0° < \theta < 180°$. The satellite transmission frequency is at 1.625 GHz. For this analysis, the received signal strength is independent of the mobile's speed, since the building is assumed of infinite extent in the direction of the mobile's travel. Depending on the satellite elevation angle θ, different ray contributions can reach the mobile. The different regions are illustrated in Fig. 1.

The ray contributions to the received signal were formulated as follows.

- $0 \le \theta \le \phi_{\rm ISB}$:
  - a) ground reflections and then second-order diffractions;
  - b) first- and second-order diffractions;
  - c) first- and second-order diffractions followed by reflections from the ground.
- $\phi_{\rm ISB} \le \theta \le \phi_{\rm RSB}$; terms a), b), and c) as above:
  - d) direct wave.
- $\phi_{\rm RSB} \le \theta \le 90°$; terms a), b), c), and d) as above:
  - e) ground reflections.
- $90° \le \theta \le \phi_{\rm RSB\,grnd}$; terms b), c), d), and e) as above:
  - f) reflections from the ground followed by diffractions from the building.
- $\phi_{\rm RSB\,grnd} \le \theta \le \phi_{\rm RSB\,bldg}$; terms b), c), d), e), and f) as above:
  - g) reflections from the building followed by reflections from the ground.

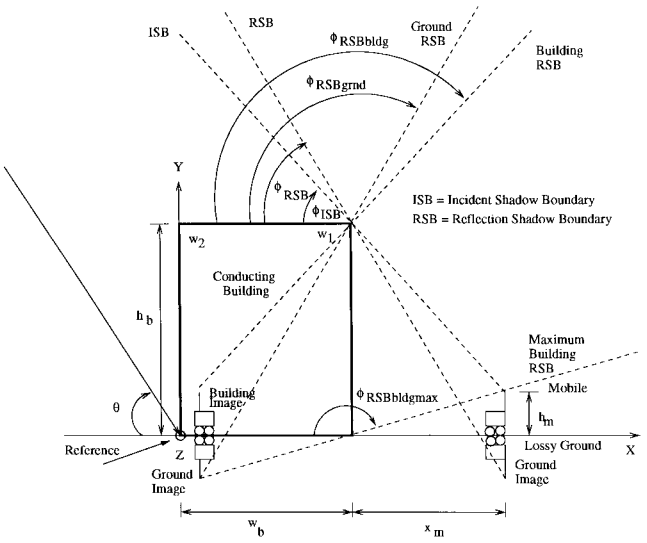

Fig. 1. Building blockage propagation model and different regions based on the satellite elevation angle.

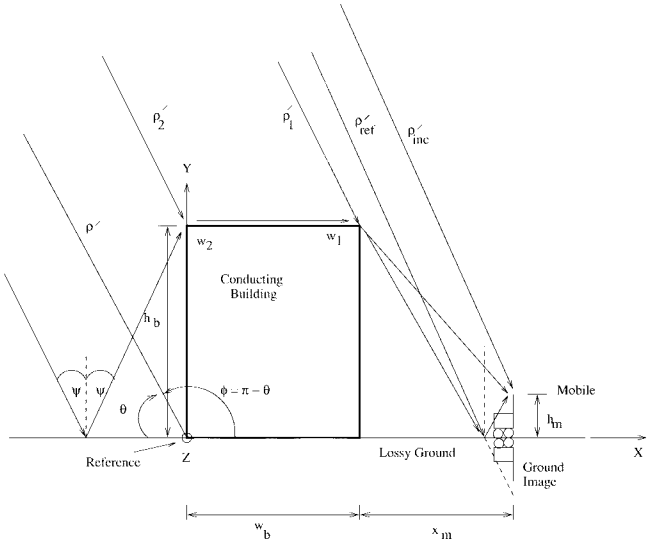

Fig. 2. Different contributions to the signal level at the mobile for angles $0 \leq \theta \leq 90°$.

- $\phi_{\mathrm{RSB\,bldg}} \leq \theta \leq \phi_{\mathrm{RSB\,bldg\,max}}$; terms b), c), d), e), f), and g) as above:
  - h) building reflections.
- $\phi_{\mathrm{RSB\,bldg\,max}} \leq \theta \leq 180°$; terms b), c), d), e), f), and h) as above:
  - i) reflections from the ground followed by reflections from the building.

In developing this propagation model, the following assumptions were made.

1) At the frequency of 1.625 GHz the building is assumed perfectly conducting.
2) The roof of the building is assumed flat and the edges form 90° corners.
3) The electrical size of the building along the z axis is assumed large (ideally infinite in extent). This is the direction that the mobile is traveling. Because of the infinite extent assumption, there will be no signal variations in the z direction. Therefore, the received signal at the mobile is independent of the mobile speed, which is assumed zero.
4) An omnidirectional antenna in the elevation plane is assumed.
5) The fields radiated by the satellite transmitting antenna impinging upon the building are locally plane waves. Also, a locally flat earth surface is assumed.

A. The Incident Waves

The first step in evaluating the diffracted fields toward the mobile is to determine the incident field at the building edges w_1 and w_2, respectively. The incident field at the two edges is expressed in terms of the incident field at the reference point. For soft (horizontal) polarization, the incident electric field is in the z direction.

The expression for the incident plane wave for soft (horizontal) polarization is

$$E_z^i(\text{reference}) = E_0 e^{-jk_0\rho'} = E_0 e^{-j\frac{2\pi}{\lambda_0}\rho'}. \tag{1}$$

The incident plane wave is evaluated at the first edge w_1 as follows:

$$E_z^i(w_1) = E_0 e^{-j\frac{2\pi}{\lambda_0}\rho_1'}. \tag{2}$$

The distance ρ_1' is related in terms of local coordinates and the distance to the reference point using the geometry shown in Fig. 2. This results in the following expression:

$$\begin{aligned} E_z^i(w_1) &= E_0 e^{-j\frac{2\pi}{\lambda_0}(\rho' - w_b\cos\phi - h_b\sin\phi)} \\ &= E_z^i(\text{reference}) \cdot e^{j\frac{2\pi}{\lambda_0}(w_b\cos\phi + h_b\sin\phi)}. \end{aligned} \tag{3}$$

In a similar way

$$E_z^i(w_2) = E_z^i(\text{reference}) \cdot e^{j\frac{2\pi}{\lambda_0}(h_b\sin\phi)}. \tag{4}$$

For satellite elevation angles greater than ϕ_{ISB} there is a direct ray contribution toward the mobile. The incident wave at the mobile with respect to the field at the reference point is given by

$$E_z^i(\text{mobile}) = E_z^i(\text{reference}) \cdot e^{j\frac{2\pi}{\lambda_0}[(w_b + x_m)\cos\phi + h_m\sin\phi]}. \tag{5}$$

For hard (vertical) polarization, the magnetic field is in the z direction. The evaluation of the incident plane wave for this polarization follows the same procedure as for soft polarization, except that the formulation is performed using the magnetic field. The expressions for the z-directed incident magnetic field at the reference point, the first edge w_1, the second edge w_2, and the mobile, respectively, are given by

$$H_z^i(\text{reference}) = H_0 e^{-j\frac{2\pi}{\lambda_0}\rho'} \tag{6}$$

$$H_z^i(w_1) = H_z^i(\text{reference}) \cdot e^{j\frac{2\pi}{\lambda_0}(w_b\cos\phi + h_b\sin\phi)} \tag{7}$$

$$H_z^i(w_2) = H_z^i(\text{reference}) \cdot e^{j\frac{2\pi}{\lambda_0}(h_b\sin\phi)} \tag{8}$$

$$H_z^i(\text{mobile}) = H_z^i(\text{reference}) \cdot e^{j\frac{2\pi}{\lambda_0}[(w_b + x_m)\cos\phi + h_m\sin\phi]}. \tag{9}$$

B. The Reflected Waves

For satellite elevation angles greater than ϕ_{RSB} there is a reflected wave from the ground to the mobile. An additional contribution that represents diffractions first from the building edges and then reflections from the ground was also included. The reflected waves at the mobile for soft and hard polarizations, respectively, with respect to the field at the reference point are

$$E_z^r(\text{mobile}) = E_z^i(\text{reference}) \cdot \Gamma^s(\psi) \cdot e^{j\frac{2\pi}{\lambda_0}[(w_b+x_m)\cos\phi - h_m \sin\phi]} \tag{10}$$

$$H_z^r(\text{mobile}) = H_z^i(\text{reference}) \cdot \Gamma^h(\psi) \cdot e^{j\frac{2\pi}{\lambda_0}[(w_b+x_m)\cos\phi - h_m \sin\phi]} \tag{11}$$

$\Gamma^{s,h}(\psi)$ is the reflection coefficient and is given by [2]

$$\Gamma^{s,h}(\psi) = \frac{\cos\psi - \frac{1}{a}\sqrt{\epsilon_r - \sin^2\psi}}{\cos\psi + \frac{1}{a}\sqrt{\epsilon_r - \sin^2\psi}} \tag{12}$$

where ψ is the incidence angle at the ground, measured with respect to the normal at the reflection point, i.e.,

$$\psi = \frac{\pi}{2} - \theta = \phi - \frac{\pi}{2}. \tag{13}$$

For typical mobile communications environments, the following ground relative permittivity was used [2]:

$$\epsilon_r = 15 - j\frac{90.0}{f\ (\text{MHz})} \tag{14}$$

where f is the frequency in megahertz. In (14), $a = 1$ for soft polarization and $a = \epsilon_r$ for hard polarization.

For satellite elevation angles greater than $\phi_{\mathrm{RSB\,bldg}}$ there is a reflected ray contribution from the building to the mobile. Additional higher order contributions, as listed previously, were also included. The building reflected waves at the mobile for soft and hard polarization, respectively, are

$$E_z^r(\text{mobile}) = E_z^i(\text{reference}) \cdot \Gamma^s(\psi) \cdot e^{j\frac{2\pi}{\lambda_0}[(w_b-x_m)\cos\phi + h_m \sin\phi]} \tag{15}$$

$$H_z^r(\text{mobile}) = H_z^i(\text{reference}) \cdot \Gamma^h(\psi) \cdot e^{j\frac{2\pi}{\lambda_0}[(w_b-x_m)\cos\phi + h_m \sin\phi]}. \tag{16}$$

If a highly conducting building is assumed (such as in our case), then the reflection coefficient for soft polarization is -1 and for hard polarization it is 1. Alternatively, a reflection coefficient similar to the one used for lossy ground can be applied to account for the finite conductivity of the building.

C. The Diffracted Waves

Diffracted contributions to the received signal at the mobile antenna are represented by first- and second-order diffractions from the two edges w_1 and w_2, respectively. The first-order diffraction term for soft polarization from edge w_1 of Fig. 3 is [6], [7]

$$E_z^d(\rho_1) = E_z^i(w_1) \cdot D^s(L, \phi_1, \phi_1', n_1) \cdot \frac{e^{-jk_0\rho_1}}{\sqrt{\rho_1}} \tag{17}$$

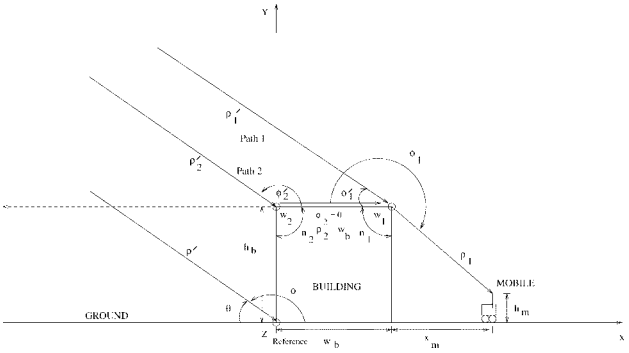

Fig. 3. Formulation of the diffracted waves from the building edges.

where $E_z^i(w_1)$, the incident field at the diffraction point w_1, is given by (3). The UTD diffraction coefficients are given by [6], [7]

$$\begin{aligned} D^{s,h}(L,\phi,\phi',n) &= -\frac{e^{-j\pi/4}}{2n2\pi}\cdot\sqrt{\lambda_0} \\ &\cdot\Bigg(\Bigg\{\cot\left[\frac{\pi+(\phi-\phi')}{2n}\right]F\left[2\pi\frac{L}{\lambda_0}g^+(\phi-\phi')\right] \\ &\quad+\cot\left[\frac{\pi-(\phi-\phi')}{2n}\right]F\left[2\pi\frac{L}{\lambda_0}g^-(\phi-\phi')\right]\Bigg\} \\ &\quad\mp\Bigg\{\cot\left[\frac{\pi+(\phi+\phi')}{2n}\right]F\left[2\pi\frac{L}{\lambda_0}g^+(\phi+\phi')\right] \\ &\quad+\cot\left[\frac{\pi-(\phi+\phi')}{2n}\right]F\left[2\pi\frac{L}{\lambda_0}g^-(\phi+\phi')\right]\Bigg\}\Bigg) \end{aligned} \tag{18}$$

where the minus sign between the curly brackets is used for soft polarization and the plus sign for hard polarization. Also, L is the distance parameter, n is the wedge index ($n_1 = n_2 = 1.5$), and $F[k_0 L g^{\mp}(\phi \mp \phi')]$ are the Fresnel transition integrals. The Fresnel integrals and their arguments are well documented in [6], [7]. A numerical algorithm for evaluating Fresnel integrals is provided in [8] and has been implemented in the developed software analysis code (C language).

The first-order diffraction term from edge w_1 is

$$E_z^d(\rho_1)|_{w_1} = E_z^i(\text{reference}) \cdot e^{j2\pi\left(\frac{w_b}{\lambda_0}\cos\phi + \frac{h_b}{\lambda_0}\sin\phi\right)} \cdot D^s(L_1, \phi_1, \phi_1', n_1) \cdot \frac{e^{-j2\pi\frac{\rho_1}{\lambda_0}}}{\sqrt{\rho_1}} \tag{19}$$

where $D^s(L_1, \phi_1, \phi_1', n_1)$ is calculated from (18). The distance parameter L, is given by

$$L = \frac{\rho\rho'}{\rho + \rho'} \tag{20}$$

where ρ is the distance from the diffraction point to the observation point, and ρ' is the distance from the source point to the diffraction point. As shown in Fig. 3, for first-order diffractions from w_1, the source point is the satellite and $\rho' = \rho_1'$, and the observation point is the mobile, thus, $\rho = \rho_1$. Since the source distance is much greater than the observation distance ($\rho' \gg \rho$) then $L_1 \simeq \rho_1$.

Note that the $\sqrt{\lambda_0}$ term in the diffraction coefficient of (18) can be incorporated into the amplitude spreading factor. This way all physical dimensions are converted into electrical quantities. The second-order diffractions from edge w_2 to edge w_1 for soft polarization are equal to zero, because $D^s = 0$ at grazing incidence.

Similarly, for hard polarization the first-order diffraction term from edge w_1 is

$$H_z^d(\rho_1)|_{w_1} = H_z^i(\text{reference}) \cdot e^{j2\pi\left(\frac{w_b}{\lambda_0}\cos\phi + \frac{h_b}{\lambda_0}\sin\phi\right)} \cdot D^h(L_1, \phi_1, \phi_1', n_1) \cdot \frac{e^{-j2\pi\frac{\rho_1}{\lambda_0}}}{\sqrt{\rho_1}}. \quad (21)$$

For the second-order diffraction term from edge w_2 to w_1, the source point is the first edge and ρ' is the distance from the first edge to the second edge, i.e., $\rho' = w_b$. The observation point is the mobile and $\rho = \rho_1$. This term can therefore be expressed as

$$H_z^d(\rho_1)|_{w_2 w_1} = H_z^i(\text{reference}) \cdot e^{j2\pi\left(\frac{h_b}{\lambda_0}\sin\phi\right)} \cdot D^h(L_2, \phi_2, \phi_2', n_2)|_{\phi_2=0} \cdot \left.\frac{e^{-j2\pi\frac{\rho_2}{\lambda_0}}}{\sqrt{\rho_2}}\right|_{\rho_2=w_b} \cdot D^h(L_{21}, \phi_1, \phi_1', n_1)|_{\phi_1'=0} \cdot \frac{e^{-j2\pi\frac{\rho_1}{\lambda_0}}}{\sqrt{\rho_1}} \quad (22)$$

where

$$L_2 \simeq \rho_2 = w_b \quad (23)$$

$$L_{21} = \frac{w_b \rho_1}{w_b + \rho_1}. \quad (24)$$

Multiple reflection–diffraction terms were included in the model, with various terms being added in different regions as previously outlined. The procedure followed when multiple reflection–diffraction terms are calculated is very similar to the one outlined in the previous sections and, due to space limitations, the derivations will be omitted in this paper. As reported by Polka *et al.* [9], terms higher than third-order are usually not necessary for accurate computations.

D. Satellite Elevation Angle versus Time

A satellite in a circular orbit 780 km above the surface of the earth, completes an orbit around the earth in 110 min. The satellite's angular speed with respect to the mobile is calculated based on the geometry illustrated in Fig. 4. Because the rays from the satellite are assumed to propagate in straight lines, an effective earth radius was used by multiplying the actual radius by 4/3, i.e., $R_e = 8488$ km [10]. The included angles γ and ϵ shown in Fig. 4 are given by

$$\gamma = \cos^{-1}\left[\frac{R_e}{R_e + R_s}\right] \quad (25)$$

$$\epsilon = \sin^{-1}\left[\frac{R_e}{R_e + R_s}\cos\theta\right]. \quad (26)$$

The objective is to relate the satellite angle β with the satellite elevation angle θ at the mobile. This is done by adding all the interior angles of the triangle OAB, i.e.,

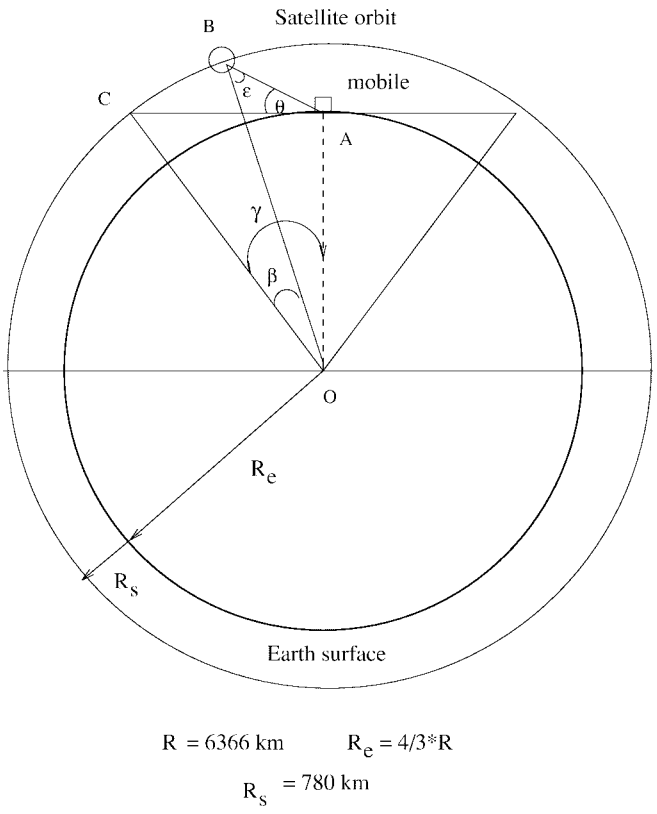

Fig. 4. Geometry for converting the satellite's angular speed reference from the center of the earth to the mobile.

$$(\gamma - \beta) + \epsilon + \left(\theta + \frac{\pi}{2}\right) = \pi. \quad (27)$$

Simplifying and substituting the values for ϵ and γ, results in

$$\beta = \theta + \sin^{-1}\left[\frac{R_e}{R_e + R_s}\cos\theta\right] + \cos^{-1}\left[\frac{R_e}{R_e + R_s}\right] - \frac{\pi}{2}. \quad (28)$$

The time variation in seconds as a function of the the elevation angle is given by

$$t = \left(\theta + \sin^{-1}\left[\frac{R_e}{R_e + R_s}\cos\theta\right] + \cos^{-1}\left[\frac{R_e}{R_e + R_s}\right] - \frac{\pi}{2}\right)\frac{110 \times 60}{2\pi}. \quad (29)$$

Therefore, the normalized signal level versus satellite elevation angle was converted to normalized signal level versus time. From these data the attenuation rate was calculated.

E. Attenuation Rate and Normalized Signal Level

The attenuation rate α is determined based on the incremental time Δ during which the normalized signal level is reduced from 0 dB to -10 dB, and is defined as

$$\alpha = \frac{10}{\Delta} \text{ dB/s}. \quad (30)$$

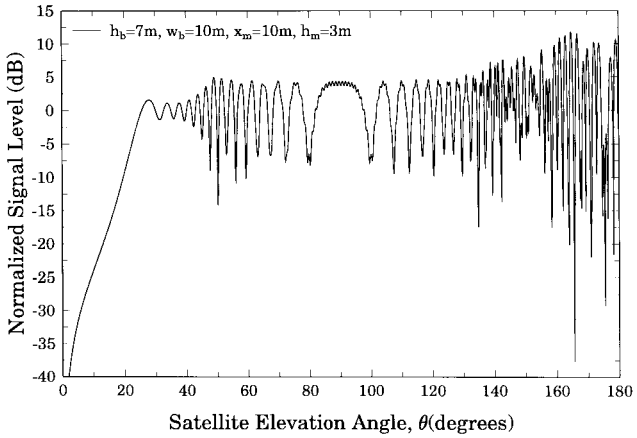

Fig. 5. One-story building in a residential area. Normalized signal level versus satellite elevation angle for soft (horizontal) polarization.

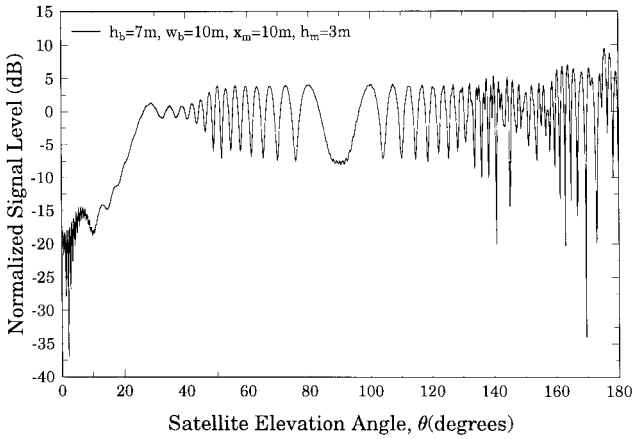

Fig. 6. One-story building in a residential area. Normalized signal level versus satellite elevation angle for hard (vertical) polarization.

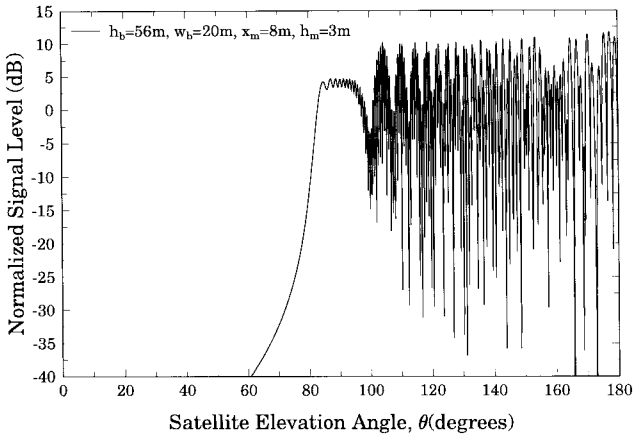

Fig. 7. Eight-story building in a moderate urban area. Normalized signal level versus satellite elevation angle for soft (horizontal) polarization.

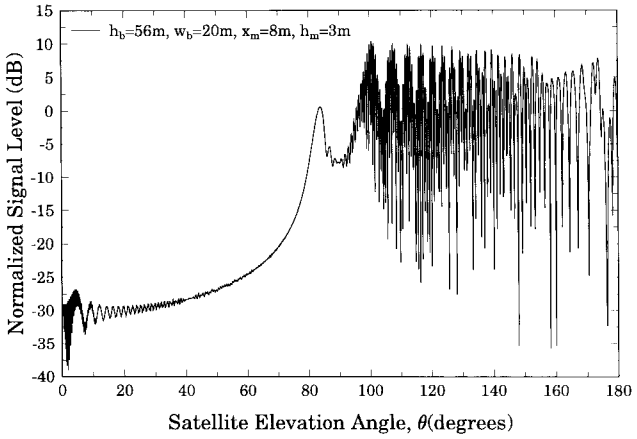

Fig. 8. Eight-story building in a moderate urban area. Normalized signal level versus satellite elevation angle for hard (vertical) polarization.

The normalized signal level is defined as

$$S^s = \left| \frac{E_z^{\text{total}}(\text{mobile})}{E_z^i(\text{reference})} \right| \tag{31}$$

$$S^h = \left| \frac{H_z^{\text{total}}(\text{mobile})}{H_z^i(\text{reference})} \right| \tag{32}$$

for soft and hard polarizations, respectively.

III. Computed Results

A. Normalized Signal Level in a Residential Environment

In a typical residential environment, buildings range from one to two stories. Computations from one-story buildings are presented. A height of 7 m and a width of 10 m for single-story buildings were used. The mobile was at a location 10 m from the building and the antenna height was 3 m. The normalized signal levels versus satellite elevation angle and versus time were computed for horizontal and vertical polarizations. Figs. 5 and 6 illustrate typical normalized signal levels for soft and hard polarizations, respectively, versus the satellite elevation angle.

For both soft and hard polarizations, $\phi_{\text{ISB}} = 21.80°$ and $\phi_{\text{RSB}} = 45.00°$ and the signal strength at 21.80° was approximately −6 dB, as expected. As calculated by the developed software code, once the satellite starts descending, it takes about 37.86 s for the signal to go from 0 to −10 dB, i.e., the attenuation rate for soft polarization is about 0.264 dB/s. For hard polarization, it takes about 46.49 s for the signal to go from 0 to −10 dB, i.e., the attenuation rate is about 0.215 dB/s. Note that the attenuation rate for hard polarization is slightly lower than for soft polarization.

B. Normalized Signal Level in a Moderate Urban Environment

In a typical moderate urban environment, buildings range from 8 to 16 stories. In this case an eight-story building was considered. The building height was 56 m and its width was 20 m, while the antenna was 3 m high and located 8 m away from the building. The normalized signal levels versus satellite elevation angle for soft and hard polarizations, respectively, are illustrated in Figs. 7 and 8.

For this typical moderate urban environment, $\phi_{\text{ISB}} = 81.42°$ and $\phi_{\text{RSB}} = 82.28°$ for both polarizations. The calculated signal strength was above −10 dB for angles greater than 80.59° for soft polarization and 79.31° for hard polarization. In this case, it took 3.63 s for the signal to drop to −10 dB

TABLE I
RESIDENTIAL (HORIZONTAL POLARIZATION)

Stories	h_b m	x_m m	ϕ°_{ISB}	ϕ°_{RSB}	θ°_{-10dB}	θ°_{0dB}	Δ s	α dB/s
1	7	10	21.80	45.00	19.60	25.65	37.86	0.264
1	7	20	11.31	26.57	9.88	14.47	47.73	0.209
1	7	30	7.59	18.43	6.30	9.83	45.03	0.222
2	14	10	47.72	59.53	45.47	50.86	13.69	0.731
2	14	20	28.81	40.36	26.94	31.82	22.81	0.438
2	14	30	20.14	29.54	18.88	22.83	26.80	0.373

TABLE II
RESIDENTIAL (VERTICAL POLARIZATION)

Stories	h_b m	x_m m	ϕ°_{ISB}	ϕ°_{RSB}	θ°_{-10dB}	θ°_{0dB}	Δ s	α dB/s
1	7	10	21.80	45.00	19.00	26.43	46.49	0.215
1	7	20	11.31	26.57	8.96	14.34	57.52	0.174
1	7	30	7.59	18.43	4.62	10.18	73.42	0.136
2	14	10	47.73	59.53	45.76	51.70	14.87	0.673
2	14	20	28.81	40.36	27.22	31.52	20.12	0.497
2	14	30	20.14	29.54	18.50	22.34	26.59	0.376

for soft polarization and 6.11 s for hard polarization, i.e., the attenuation rates were 2.753 dB/s and 1.635 dB/s, respectively.

C. Statistics in a Residential Environment

For residential environments, statistics were accumulated for both one- and two-story buildings with the distance from the mobile to the building ranging from 10 to 30 m in 10-m increments. Single-story buildings were assumed to be 7-m high and two-story buildings 14-m high. The values of the attenuation rate for horizontal polarization are shown in Table I and those for vertical polarization in Table II. For the results shown in Tables I and II, the building width was 10 m and the antenna height was 3 m.

The first column in the Tables I and II, corresponds to the number of stories in the building, the second column is the building height h_b (in meters), and the third column the distance from the mobile to the building x_m (in meters). $\phi_{\rm ISB}$ is the minimum angle (in degrees) at which the direct signal from the satellite can be received by the mobile antenna and $\phi_{\rm RSB}$ the minimum angle (in degrees) at which a reflection from the ground is also received by the mobile antenna. $\phi_{\rm ISB}$ and $\phi_{\rm RSB}$ are shown in Fig. 1. Also, $\theta_{-10\,\rm dB}$ and $\theta_{0\,\rm dB}$ are the satellite elevation angles (in degrees) at which the received signal is -10 and 0 dB, respectively. Δ is the elapsed time (in seconds) for the signal to go from 0 to -10 dB, and α is the attenuation rate (in decibels per second).

The values of the attenuation rate in Tables I and II were averaged to obtain the mean attenuation rate for residential environments, which is given in Table III and was found to be 0.359 dB/s. Further, the mean values of $\phi_{\rm ISB}$, $\phi_{\rm RSB}$, $\theta_{-10\,\rm dB}$, $\theta_{0\,\rm dB}$, Δ, and α for residential environments are also listed in Table III. As illustrated in Table III, on average the mobile antenna receives a direct satellite signal for elevation angles above 22.90°, and a reflected signal from the ground for elevation angles above 36.57°. The average satellite elevation angle for which the normalized signal level is -10 dB is 20.93° while the corresponding angle at which the normalized signal level is 0 dB is 26.00°.

TABLE III
MEAN RESIDENTIAL PARAMETERS

ϕ°_{ISB}	ϕ°_{RSB}	θ°_{-10dB}	θ°_{0dB}	Δ s	α dB/s
22.90	36.57	20.93	26.00	36.08	0.359

TABLE IV
MODERATE URBAN (HORIZONTAL POLARIZATION)

Stories	h_b m	x_m m	ϕ°_{ISB}	ϕ°_{RSB}	θ°_{-10dB}	θ°_{0dB}	Δ s	α dB/s
8	56	8	81.42	82.28	80.59	82.90	3.63	2.753
8	56	12	77.24	78.50	76.49	81.96	8.72	1.147
8	56	16	73.20	74.83	71.95	74.40	4.08	2.455
12	84	8	84.36	84.75	83.07	85.08	3.13	3.193
12	84	12	81.57	82.15	80.89	82.81	3.02	3.316
12	84	16	78.83	79.58	78.92	82.36	5.44	1.839
16	112	8	85.80	86.02	84.59	86.34	2.71	3.687
16	112	12	83.72	84.04	82.64	84.40	2.74	3.648
16	112	16	81.65	82.08	81.06	82.74	2.65	3.778

TABLE V
MODERATE URBAN (VERTICAL POLARIZATION)

Stories	h_b m	x_m m	ϕ°_{ISB}	ϕ°_{RSB}	θ°_{-10dB}	θ°_{0dB}	Δ s	α dB/s
8	56	8	81.42	82.28	79.31	83.19	6.11	1.635
8	56	12	77.24	78.50	75.44	78.31	4.64	2.154
8	56	16	73.20	74.83	71.98	77.48	9.04	1.106
12	84	8	84.36	84.75	83.88	95.16	17.49	0.572
12	84	12	81.57	82.15	79.89	82.83	4.62	2.163
12	84	16	78.83	79.58	76.88	79.50	4.20	2.382
16	112	8	85.80	86.02	85.92	94.60	13.41	0.746
16	112	12	83.72	84.04	83.03	95.62	19.48	0.513
16	112	16	81.65	82.08	80.21	82.66	3.85	2.600

TABLE VI
MEAN MODERATE URBAN PARAMETERS

ϕ°_{ISB}	ϕ°_{RSB}	θ°_{-10dB}	θ°_{0dB}	Δ s	α dB/s
80.86	81.58	79.82	84.02	6.63	2.205

D. Statistics in a Moderate Urban Environment

For a moderate urban environment, statistics were accumulated for building heights 8 to 16 stories in four-story increments. The distance from the mobile to the building ranged from 8 to 16 m in 4-m increments. For these statistics the building width was 20 m and the antenna height 3 m. The results are shown in Tables IV and V for horizontal and vertical polarizations, respectively.

The values of $\phi_{\rm ISB}$, $\phi_{\rm RSB}$, $\theta_{-10\,\rm dB}$, $\theta_{0\,\rm dB}$, Δ, and α in Tables IV and V were averaged to obtain mean values for moderate urban environments, as shown in Table VI. The mean value of the attenuation rate was found to be 2.205 dB/s and, on average, the mobile antenna receives a direct satellite signal for elevation angles above 80.86° and a reflected signal for elevation angles above 81.58°. Further, the average satellite elevation angle for which the normalized signal level is -10 dB is 79.82°, and the corresponding angle at which the normalized signal level is 0 dB and 84.02°.

Note that due to the nonlinear relationship between the satellite elevation angle and time and the fact that the attenuation rate was calculated based on the 0 to -10 dB threshold values, a consistent trend in the values of the attenuation rate

cannot be established. Thus, to explain each calculated value of the tabulated attenuation rates, one has to examine each case individually and determine at which angles the signal is 0 and -10 dB, respectively, with respect to the values of ϕ_{ISB} and ϕ_{RSB}. For this, plots of the normalized signal level versus both satellite elevation angle and time are useful. However, only a representative number of such plots versus elevation angle were included in this paper.

IV. Conclusion

A propagation model for building blockage in satellite mobile communication systems has been presented. This model was applied to characterize the satellite signal received by an omnidirectional antenna when the signal path is blocked by a row of buildings. This model has been based on high-frequency ray-tracing methods and includes diffractions from the building edges, reflections from the ground and building, and the direct wave. Also, higher order interactions have been added in the model. The normalized signal level at the mobile antenna is calculated versus the satellite elevation angle and time, based on the satellite angular speed around the earth. Examples of normalized signal levels and attenuation rates were computed for residential and moderate urban environments.

When the satellite begins to descend behind a building, the signal level obtained from this analysis was approximately -6 dB, which the reader can verify by observing the signal strength at ϕ_{ISB} from the plotted cases of normalized signal level versus satellite elevation angle. Also, it was found that the mean attenuation rate increases from 0.359 to 2.205 dB/s as one moves from residential to moderate urban environments, i.e., the signal deteriorates much faster in moderate urban environments than in residential environments. The average angle at which the normalized signal level falls off to -10 dB was 20.93° for a typical residential environment and 79.82° for a typical moderate urban environment. This suggests that the possibilities of having a normalized signal level higher than -10 dB are much smaller in a moderate urban environment when compared to a residential environment.

Acknowledgment

The authors would like to thank Dr. M. Frank of Motorola, Inc., Satellite Communications Division, Chandler, AZ, for his continued interest and support of this project.

References

[1] F. Ananasso and F. D. Priscoli, "The role of satellites in personal communication services," *IEEE J. Select. Areas Commun.*, vol. 13, pp. 180–196, Feb. 1995.

[2] H. L. Bertoni, W. Horcharenco, L. R. Maciel, and H. H. Xia, "Propagation prediction for wireless personal communications," *Proc. IEEE*, vol. 82, pp. 1333–1359, Sept. 1994.

[3] W. J. Vogel and U. Hong, "Measurement and modeling of land mobile satellite propagation at UHF and L-band," *IEEE Trans. Antennas Propagat.*, vol 36, pp. 707–719, May 1988.

[4] W. J. Vogel, G. W. Torrence, and H. Lin, "Simultaneous measurements of L- and S-band tree shadowing for space-earth communications," *IEEE Trans. Antennas Propagat.*, vol. 43, pp. 713–719, July 1995.

[5] R. Akturan and W. J. Vogel, "Optically derived elevation angle dependence of fading for satellite PCS," in *Proc. NAPEX XIX ACTS Propagat. Studies Workshop*, Ft. Collins, CO, June 1995.

[6] R. Kouyoumjian and P. Pathak, "A uniform geometrical theory of diffraction for an edge in a perfectly conducting surface," *Proc. IEEE*, vol. 62, pp. 1448–1461, Nov. 1974.

[7] C. A. Balanis, *Advanced Engineering Electromagnetics*. New York: Wiley, 1989.

[8] J. Boersma, "Computation of Fresnel integrals," *J. Math. Comput.*, vol. 14, p. 380, 1960.

[9] L. A. Polka, C. A. Balanis, and A. C. Polycarpou, "High-frequency methods for multiple diffraction modeling: Application and comparison," *J. Electromagn. Waves Appl.*, vol. 8, nos. 9/10, pp. 1223–1246, 1994.

[10] C. A. Balanis, *Antenna Theory Analysis and Design*, 2nd ed. New York: Wiley, 1996.

Panayiotis A. Tirkas (S'89–M'93), for photograph and biography, see p. 266 of the February 1998 issue of this TRANSACTIONS.

Chad M. Wangsvick (S'92–M'98) received the B.S. degree from Colorado State University, Fort Collins, in 1994, and the M.S. degree from Arizona State University, Tempe, in 1997, both in electrical engineering.

From 1995 to 1997, he was a Graduate Research Assistant in the Department of Electrical Engineering, Telecommunications Research Center, Arizona State University, involved in the investigation of satellite-to-mobile communication in various propagation environments. He is currently a member of the technical staff in the Defense Systems Segment of Raytheon Systems Company, Tucson, AZ, working on antennas for exo-atmospheric flight, as well as multiband antennas.

Constantine A. Balanis (S'62–M'65–SM'74–F'86), for photograph and biography, see p. 259 of the February 1998 issue of this TRANSACTIONS.